Rapid Stress Relaxation of High T_g Conjugated Polymeric Thin Films

Guorong Ma[1], Song Zhang[1], Luke A. Galuska[1], Xiaodan Gu[1]*

1. School of Polymer Science and Engineering, The University of Southern Mississippi, Hattiesburg, MS, 39406, USA

Correspondence to: Xiaodan Gu (Email: xiaodan.gu@usm.edu)

Abstract

Conjugated polymers consist of complex backbone structures and side-chain moieties to meet various optoelectronic and processing requirements. Recent work on conjugated polymers has been devoted to studying the mechanical properties and developing new conjugated polymers with low modulus and high crack onset strain, while the thin film mechanical stability under long-term external tensile strain is less investigated. Here we performed direct mechanical stress relaxation tests for both free-standing and thin film floated on water surface on both high-T_g and low-T_g conjugated polymers, as well as a reference non-conjugated sample, polystyrene. We measured thin films with a range of film thickness from 38 nm to 179 nm to study the temperature and thickness effect on thin film relaxation, where an apparent enthalpy–entropy compensation effect for glassy polymer PS and PM6 thin films was observed. We also compared relaxation times across 3 different conjugated polymers and showed that both crystalline morphology and higher modulus reduce the relaxation rate besides higher glass transition temperature. Our work provides insights

into the mechanical creep behavior of conjugated polymers, which will have an impact on the future design of stable functional organic electronics.

Keywords: polymer thin film, stress relaxation, confinement effect, glass transition temperature, conjugated polymers

Introduction

Various organic electronic devices like organic-field-effect transistors (OFETs), organic thermoelectric and organic photovoltaics (OPV) are using conjugated polymers (CPs) as their active layer. [1] For the past few years, many CPs have been studied extensively to explore their potential as flexible electronics, due to their unique ability to transfer charges while being mechanically flexible.[2] CPs have a complex backbone and side-chain moieties to allow versatile control of its electronic and mechanical properties,[3-5] resulting in a broad range of glass transition temperatures (T_g).[6-8] It has been reported that side-chain length can greatly influence chain dynamics[9-11] in the thin-film state, where the dynamics of the backbone are greatly accelerated by the longer alkyl sidechains. During the device operation, particularly in thin film devices, prolonged deformation can occur. This sustained external stress induces alterations in chain conformation and film morphology, ultimately resulting in a decline in performance. Consequently, there is a critical need to assess the stability of the device under external stress conditions. Despite those works, there is little study to understand the relaxation behavior of conjugated polymeric film under tensile load. However, the knowledge of CP thin film's mechanical behavior under external loads could be leveraged to improve the stability of various organic electronic devices under mechanical stress.

It is widely observed that thin film's properties could differ with bulk as film thickness decreases (e.g. for film within 10s of nm). It can be the T_g[12-15], and Young's modulus.[16] For a free-standing thin film, the reduction of T_g can be explained by having two highly mobile layers near the film-air interface.[17-22] For the supported thin film, various substrates interacting with the film could also alter chain dynamics, as demonstrated in previous studies on silicon[23], silicon oxide[24-27], polydimethylsiloxane[28], poly(methyl methacrylate)[29], ionic liquid[30] and water.[16, 31]

Many experimental techniques have been developed to probe the polymer chain dynamics in thin films, especially for the model system polystyrene (PS) thin film. Using X-ray reflectivity, Yang *et al*.[32] found that for the ultrathin PS film, the relaxation can happen even at room temperature, indicating the substrate absorbs polymer chains and reduces the film dynamics. Akabori *et al.*[24] used supported dynamic mechanical analysis (DMA) to show that the free surface and the substrate interface can have contrasting effects on PS film dynamics. However, Lu *et al.*[30] demonstrated that thin PS films with thicknesses below 100 nm floated on the ionic liquid have T_g values similar to that in the bulk, independent of initial film thicknesses. Hanakata *et al.*[33] performed molecular dynamics simulations to systematically investigate the influence of solid substrate properties on relaxation in supported polymer films and found that substrate identity significantly influences overall thin film chain dynamics. Torkelson *et al.*[34-35] used ellipsometry and fluorescence methods to investigate the confinement effect and found that the dynamic heterogeneity is more obvious in glassy thin films. These extensive experiments and sometimes contradicting results reflect the dynamic heterogeneity nature of the glassy polymer chain in thin films. While these studies provide good predictions for behaviors of linear glassy chain dynamics, the elucidation of the stress relaxation of the entire polymer films is lacking. A highly mobile layer

is shown to cause the thin film to relax below T_g, however, how deep can this surface influence the film is less considered.[34-35]

Due to the fragile nature of thin films, applying tensile tests on polymer thin films (below 100 nm) can be challenging. Atomic Force Microscopy (AFM) has been widely used to measure partial topography relaxation[36] or structure recovery through nanoindentation at the thin film surface. Apart from the microscopy tool, Chung *et al.*[28] reported a thin PS film relaxation measurement using buckling metrology supported on a PDMS substrate. They used a stretched exponent equation to model the stress relaxation process and found Arrhenius-type temperature-dependent relaxation time and an apparent entropy-enthalpy compensation behavior, which were in accordance with the simulation predictions.[33] This further demonstrated the dynamic heterogeneity of chain dynamics at different depths in the thin glassy film. Chan *et al*.[37] used a thermal wrinkling method to show the viscoelastic nature of thin PS film caped by silicon and aluminum substrates ranging from 642 nm to 74 nm above PS glass transition temperature. Despite mature literature on thin film relaxation of PS films, up to date, direct probing the stress relaxation for stretched conjugated polymeric thin film has not been reported.

In this work, we reported the first in-depth stress relaxation behavior study of sub-100nm supported and free-standing conjugated polymer thin films. Recently, we have developed a new method to achieve the uniaxial tensile test with either film floated on water or fully free-standing film, and probe the elastic modulus and fracture behaviors on thin films.[31, 38] By incorporating a heating element and water compensation system here, we now can track the stress relaxation of polymer thin films with different thicknesses and at different temperatures. By monitoring the time evolution of the stress dissipation in polymeric thin films, we can measure the relaxation process, model the stress relaxation, and understand its underlying mechanism. We further conducted the

relaxation measurement on free-standing films to further remove the water bath effect, using a thin film transfer method that our previous work reported by the shear motion transfer process.[39] We systematically investigated the role of film thicknesses and temperatures in the relaxation behavior of conjugated polymeric films. Our study involved polystyrene (PS), PBDB-T-2F (PM6), poly(9,9-didecylfluorene) (PFO-C10), and poly[2,5-(2-octyldodecyl)-3,6-diketopyrrolopyrrole-alt-5,5-(2,5-di(thien-2-yl)thieno [3,2-b]thiophene)] (PDPP-TT). Using our unique setup, we were able to expand upon our previous understanding of how polymer chain dynamics is affected in various thin film systems by studying the influence of temperature and thickness on the relaxation process of the aforenoted CPs. Interestingly, low T_g polymer showed stress fast relaxation and it further hastened upon thin film confinement. Surprisingly, we discovered that despite a similar apparent backbone T_g, PM6 relaxed much faster than its non-conjugated peer polymer, PS. The finding suggests that local heterogeneity between the backbone and alkyl sidechain is an important consideration for stress relaxation for conjugated polymer thin films.

Experiment

1. Materials

PS (Polymer Source, number averaged molecular weight M_n = 173 kg/mol, Dispersity $Đ$ = 1.06), PBDB-T-2F (PM6) (Ossila, M_n = 28 kg/mol, $Đ$ = 2.46) and PDPP-TT (Ossila, M_n = 29.6 kg/mol, $Đ$ = 3.36) were used as received. PFO-C10 (M_n = 36 kg/mol, $Đ$ =3.29) was synthesized in-house according to the previously reported method. PDMS (Dow Corning Sylgard 186) was mixed at a ratio of 10:1 and cured at 50 ℃ overnight. All the solvents were from Thermo Scientific and used as received.

2. Sample preparation

Thin films were prepared via spin-casting (5-30 mg/mL PS, 10-20 mg/mL conjugated polymers) onto poly (sodium 4-styrenesulfonate)-(PSS)-coated silicon wafers. The wafer was oxygen plasma etched before spin coating to clean the surface and form a hydrophilic surface.[40] Thin film samples were then vacuum annealed for over 10 hours above their respective T_g values (130 ℃ for PS and PM6, 50 ℃ for PFO-C10 and PDPP-TT) to remove any possible residual solvents, as well as to eliminate internal stress accumulated during spin coating.[15, 41] Films were then cooled down to room temperature at a rate of 1 ℃/min to prevent thermal stress accumulation. Lastly, films were laser patterned into a dog-bone shape with a gauge length of 8 mm and a width of 2 mm.

3. Thin-film stress relaxation test on a pseudo-free standing tensile tester

The pseudo-free tensile test with temperature control was based on a customizable thin-film tensile tester.[31] For this testing system, specimens were manually floated onto deionized (DI) water and then attached to a high-precision load cell and linear stage. The specimen was grabbed by two rectangular PDMS (10:1 ratio) pads with a dimension of 6 × 8 mm. Experimentally crosslinked PDMS showed no stress relaxation (Figure S1), and it was treated as an elastomeric species in the tensile test as the literature mentioned.[42] After equilibration at the desired temperature, a small strain of 0.8% was applied to a thin film with a strain rate of 5 x 10^{-3} s^{-1}. Stress recording started simultaneously. The force on the sample was recorded at a rate of 2 Hz, with an initial force determined through the value of maximum force. The temperature of the water was controlled through a temperature controller. The maximum water temperature accessible in this work was limited to 50 ℃ to reduce water condensation onto the instrument. The water surface was maintained at the same height level throughout the test by replenishing water back into the water bath using a syringe pump, in order to compensate for the evaporation of water at elevated temperatures. The water evaporation rate was measured independently and used here.

4. Free-standing thin-film stress relaxation test

The free-standing tensile tester is described in detail in our previous published works through a unique thin film shear transfer process to move the film from water surface to air to form sub-100nm freestanding film.[39] The temperature for the free-standing thin film tensile test was controlled using a temperature-controlled chamber (see Figure S2).

5. Film thickness measurement

The film thickness of prepared polymer thin films was measured via an interferometer (Filmetrics F20-UVX) and an AFM (Cypher Asylum AFM) respectively. Thickness was averaged over three different measured areas.

Result and discussion

Table 1 Summary of molecular weight, dispersity, glass transition temperature T_g, and sidechain mass fraction of polymers used in this study.

Name	M_n (kg/mol)	$Đ$	T_g (°C)	sidechain mass fraction
PS	173	1.06	105	--
PM6	28	2.46	138	0.36
PDPP-TT	30	3.36	3*	0.54
PFO-C10	36	3.29	73	0.59

* Adopted from ref 43.

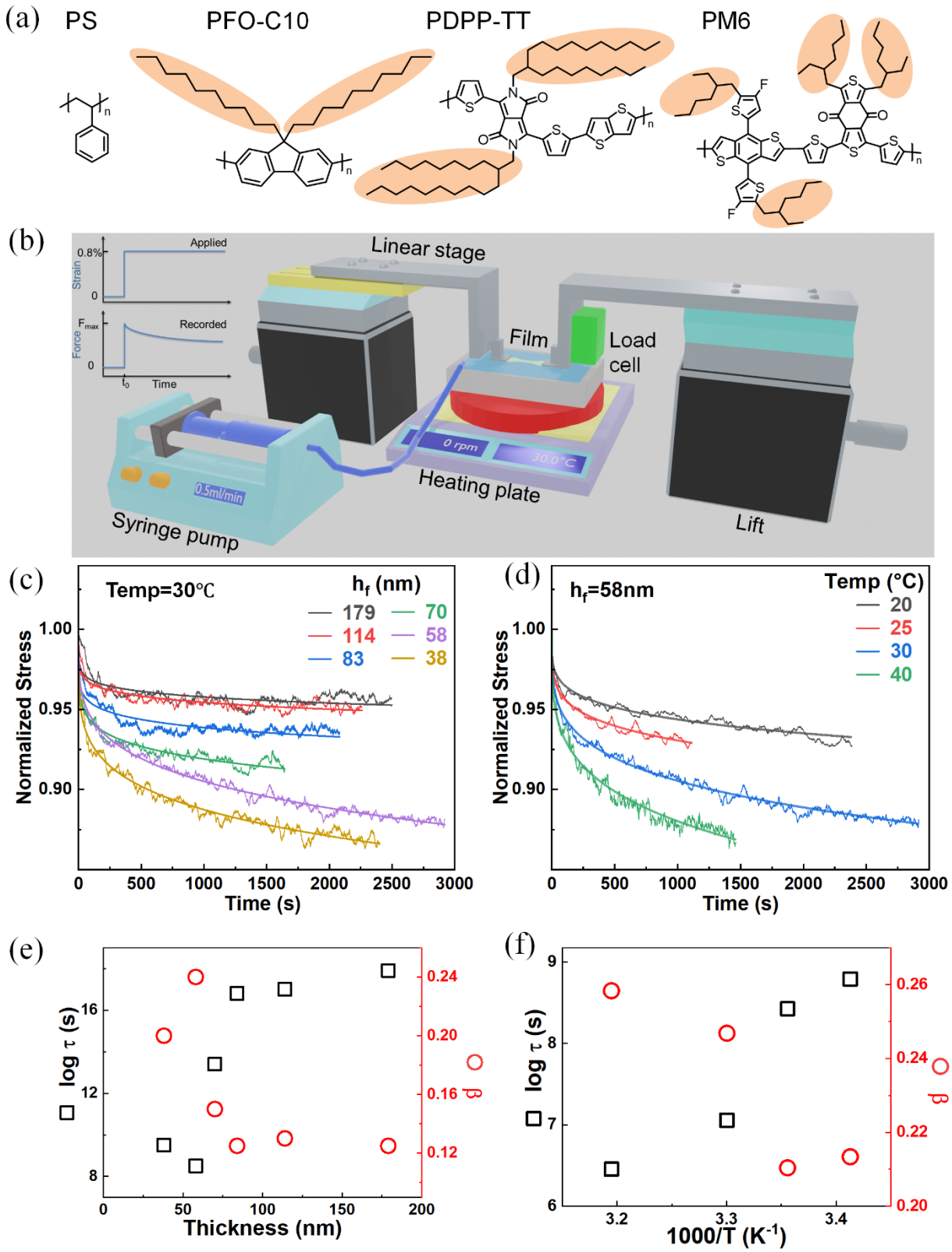
(a)
PS
PFO-C10
PDPP-TT
PM6
(b)
Applied
Strain
0.8%
0
Recorded
Force
Time
Linear stage
Film
Load cell
0 rpm
30.0°C
Heating plate
0.5ml/min
Syringe pump
Lift
(c)
Temp=30℃
h_f (nm)
179
114
83
70
58
38
Normalized Stress
Time (s)
(d)
h_f=58nm
Temp (°C)
20
25
30
40
Normalized Stress
Time (s)
(e)
log τ (s)
β
Thickness (nm)
(f)
log τ (s)
β
1000/T (K^{-1})

Figure 1 Representative stress relaxation setup and results for polymer thin films. (a) Chemical structures of four polymers (1) PS, (2) PFO-C10, (3) PDPP-TT, and (4) PBDB-T-2F (PM6). Sidechains are highlighted with orange shadows. (b) The apparatus of the pseudo-free standing tensile tester with a hot stage at the bottom of the water bath and a syringe pump on the left to replenish the evaporated waters. The insert shows typical stress relaxation data. (c) Representative raw result (wavy curve) and KWW equation fitting curve (smooth curve) for PS films with different thicknesses at 30 ℃ (c) and 58 nm films (d) at different temperatures. Fitting parameters as a function of film thickness (e), based on data (c) and temperature (f), based on data (d), where τ is the relaxation time (black square), and β is the stretching exponent (red circle).

We first validated our measurement technique on the model PS thin film and examined the thickness and temperature effect on the thin-film relaxation behavior. Our stress relaxation measurement was directly performed on dog-bone-shaped thin films floating on the water (**Figure 1b)**. Permanent plastic deformation was prevented by applying a small strain (0.8%) that is below its yield strain (**Figure S4**). The force on the films dropped after the stretch and continued to decrease. To quantify stress relaxation, the force on the film was normalized by the maximum force $F_{normalized} = F/F_{max}$, where the F_{max} is the maximum force on the sample upon stretching. Traditionally, stress relaxation in supercooled liquids can be described by Kohlrausch–Williams–Watts (KWW) function[28, 32, 44-45]

$$F_{normalized}(t) = \exp\left[-(t/\tau)^{\beta}\right] \quad (1)$$

where τ is the relaxation time, and β is the stretching exponent varying from 0 to 1[46]. As shown in **Figure 1c,** all relaxation curves for PS thin film fit well to KWW equation over a long time

scale. It is also noticed that the stress relaxation increased below 100 nm when the film is under a confined state. The phenomenon of fast chain dynamics upon confinement agreed well with other reports using the thin film buckling technique from thin film on top of PDMS substrate.[28] It's important to highlight that data from the long-time range holds more weight in the fitting process compared to data from the short-time range. This is primarily due to the larger volume of data available, which makes short-time range fitting less optimal. The observed noise in short-time data can be attributed to the inertia of the load cell, a phenomenon that is more pronounced at elevated temperatures. This effect is particularly significant as film thickness decreases or temperature rises. For example, it was reported that the T_g of PS films decreases significantly below 80 nm[47], implying a faster stress relaxation rate than bulk. To quantify the relaxation kinetics, we examined the film thickness and temperature effect on τ and β, as shown in **Figure 1e and 1f**. A steady increase of β as thickness decreases/temperature increases has been demonstrated previously[28, 48], which was attributed to a reduction of dynamic heterogeneity within the polymer sample[49]. Such heterogeneity decrease originates from a highly mobile layer on the glassy film and air interface.[21, 50] At higher temperatures, the mobility of polymer chain segments is enhanced, thus τ decreases drastically, for example, for 70 nm thin PS films the relaxation time τ decreases from 3.6×10^{10} s to 3.2×10^{6} s when temperature increases from 20 ℃ to 50 ℃ (**Figure S6**). This effect can be attributed to the increase in the volume of the mobile layer.[17] For example, the relaxation time τ dropped for 7 orders of magnitudes from 114 nm to 38 nm films at 30 ℃ (**Figure 1e**). Thus, we demonstrated and validated a new reliable technique that can directly probe the stress relaxation for thin-film samples down to 40 nm.

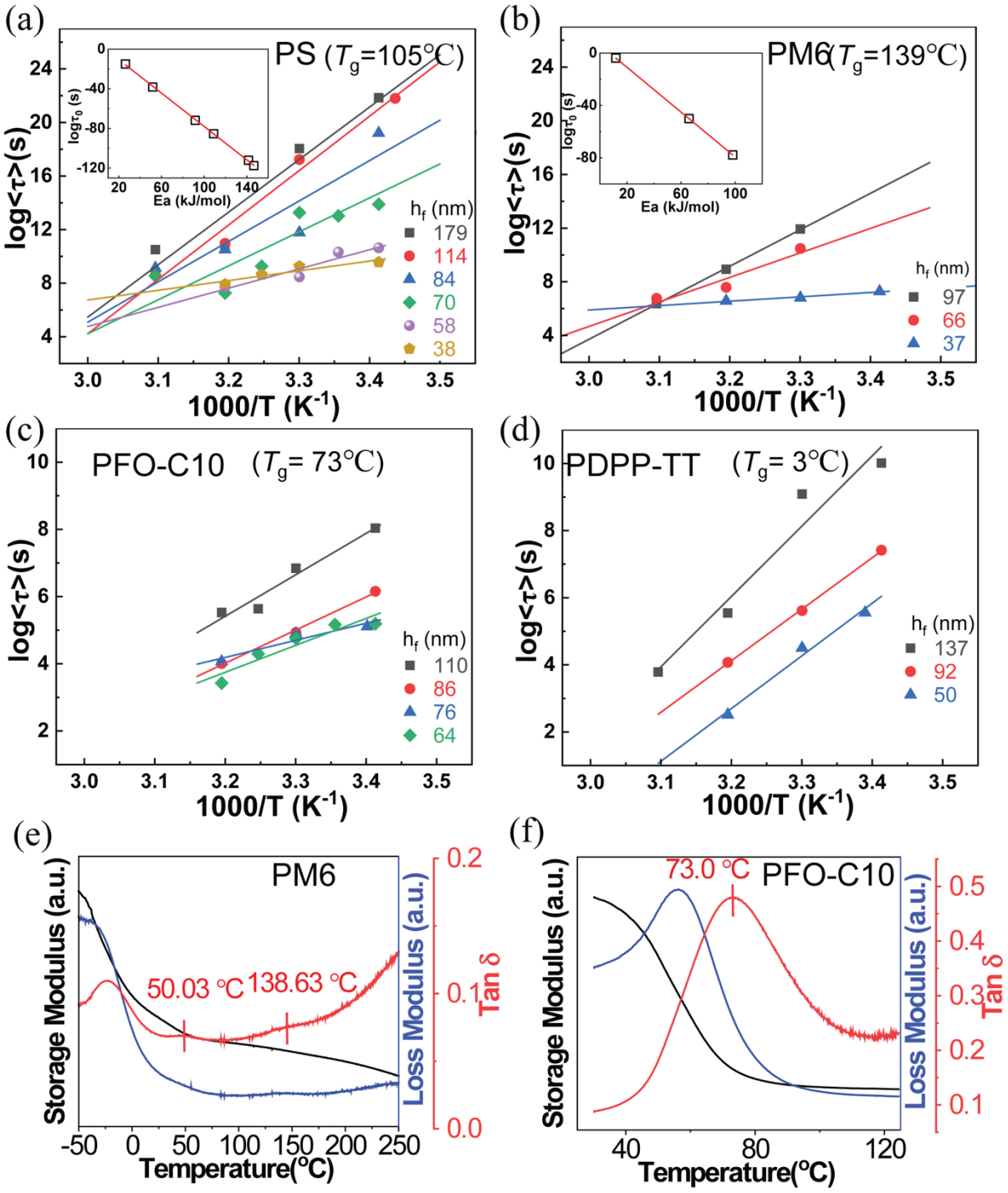

Figure 2 Arrhenius behavior of relaxation time as a function of film thickness and temperature for (a) PS (b) PM6 (c) PFO-C10 and (d) PDPP-TT with their T_g values. The inset plot shows τ_0 and

the activation energy, obtained from the intercept and slope of the fitting straight lines, respectively. The DMA measurement results for the $T_g s$ of the PM6 (e), and PFO-C10 (f) polymer respectively.

After validating our methodology on the PS thin film, we selected three representative CPs that were previously used in OPV, OLED, and OFET respectively, including PBDB-T-2F (PM6), PFO-C10, and PDPP-TT. Their T_g values were determined by DMA (**Figure 2**e, f and **Table 1)**. In bulk polymer systems, temperature-dependent relaxation behavior follows a linear Arrhenius relationship. Such an Arrhenius-type temperature dependence has been previously observed in thin glassy polymer films.[51-52] We applied a relaxation time correction using **Eq. 2**:

$$\langle\tau\rangle = \int_0^{+\infty} exp\left[-(t/\tau)^{\beta}\right] dt = \tau\Gamma(1/\beta)\beta \quad (2)$$

This correction produces an averaged relaxation time ⟨τ⟩ as described by previous reports[53] where Γ is the Gamma function, and β is the stretching exponent. Relaxation time can be described as a function of film thickness h_f and temperature T,[28] which can be written as:

$$\langle\tau\rangle(h_f, T) = \tau_0(h_f)e^{-E_a(h_f)/RT} \quad (3)$$

where τ_0 is a prefactor, E_a is the activation energy for the relaxation process, and R is the gas constant. The strength of temperature dependence on relaxation time becomes weaker as film thickness decreases, evidenced by the decrease of slope of the straight line. It is noticed that as film thickness decreases, τ decreases linearly in all Arrhenius plots (**Figure 2**). Meanwhile, the temperature influence on relaxation time τ becomes weaker in thinner films, leading to a drop in E_a. This is expected as film polymer segments are close to the highly mobile surface in confined film.

By comparing these four polymers, PS and PM6 showed a converging trend for different film thicknesses, or there exists a common temperature, T_{comp}, where films of varying thicknesses have comparable relaxation times (**Figure 2a, b**). This can be verified by plotting the intercept and slope of the fitting lines which follow a linear trend, as shown in the inset. This common temperature was typically referred to as the enthalpy–entropy compensation temperature, which had been observed in previous experiments through the film-on-elastomer method.[28] Theoretical studies also showed that T_{comp} was usually close to the T_g of bulk glassy materials.[54] However, it should be noted that the observed T_{comp} for PS is 60 ± 3 ℃, which is below its T_g of 100 ℃.[55] Such inconsistency could result from the influence of water substrate on the polymer chain dynamics during stress relaxation. Liquid water is considered a soft substrate, and it could plasticize the polymer and accelerate the local polymer chain dynamics at the polymer-water interface.[41, 56] Previously, the presence of water in the thin PS film was confirmed by quartz crystal microbalance (QCM) and neutron reflectivity.[39] It is expected that this slow water saturation process leads to various water absorption levels at different temperatures, leading to an apparent lower T_{comp}. Such T_g approach from T_{comp} is from water swelling dynamics rather than thermodynamics, which has a different sensitivity to the polymer-substrate interaction and dynamic heterogeneity in the glassy thin film.[57] In other words, the thin highly mobile layer contributes less to the thermodynamic properties of the thin film, but will significantly affect the dynamics of the whole glassy film. Similar depression of T_{comp} also occurs with another high-T_g polymer, PM6, where T_{comp} is 54 ± 2 ℃. This mismatch between T_{comp} and T_g is similarly due to the relatively fast chain dynamics for thin-film surfaces upon interaction with water. On the other hand, for low-T_g CP samples (<40 ℃ [43, 58]) like viscoelastic PFO-C10 and PDPP-TT, there is no converging trend at different

thicknesses. Their fast chain dynamics at ambient temperature result in a lack of enhanced surface highly mobile layer which only exists in glassy films (**Figure 2c, 2d**), as proved by other study.[35]

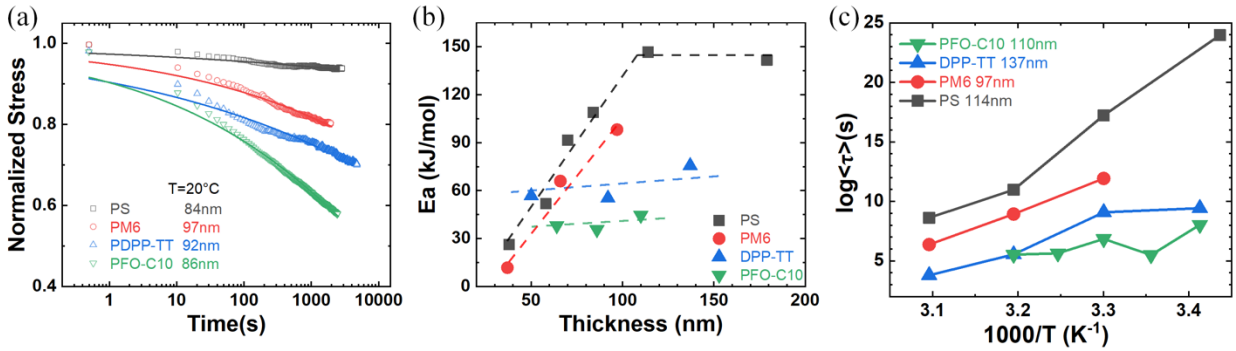

Figure 3 Comparison of relaxation behaviors between four polymers. (a) Stress relaxation evolution for films at around 90 nm. (b) Activation energy as a function of film thickness for all four polymers. (c) The temperature effect on relaxation time for thick films (above 90 nm).

Figure 3a plotted the stress relaxation of ~ 90 nm thick films to compare relaxation behaviors for four polymers. As expected, the stress relaxation was faster in PFO-C10 and PDPP-TT than PS due to their low T_g. Although PM6 exhibited a higher backbone bone T_g (e.g. 138 ^{0}C) than PS, stress relaxation for stained PM6 film happened faster than PS, which can be attributed to structural heterogeneity, and low elastic modulus (**Figure S4**). Keep in mind that the PM6 not only has a high T_g backbone, but also a significant amount (e.g. 36% by weight) of low T_g alkyl sidechains. The sidechains with much fast-dynamic can accelerate the backbone dynamics verified by simulation[59] and experiment[35].

The PFO-C10 and PDPP-TT systems exhibited the most prominent chain relaxation in this study due to their low T_g in both the backbone and sidechain (**Figure 3a**). They are also softer based on the thin film tensile testing result (**Figure S4**). Compared to PM6 polymer, the long, flexible side chains in PFO and PDPP-TT polymer further lowered the backbone T_g and hastened the backbone

dynamic, allowing polymer chains to slide past each other.[10, 60] While PFO-C10 has a higher T_g than PDPP-TT, the relaxation is also faster. This can be explained by the microstructure in the thin film. As shown by grazing-incidence wide-angle X-ray scattering (GIWAXS) (**Figure S5)**, PFO-C10 is a relatively amorphous polymer after spin coating. In contrast, PDPP-TT shows multiple higher-order lamellar stacking peaks, indicating its semicrystalline nature. The contribution from tie chains connecting crystalline domains in PDPP-TT polymer here is responsible for slowing the overall relaxation of amorphous chains compared to the PFO polymers. Overall, the relaxation process interplay between T_g, degree of crystallinity, and elastic modulus of the polymers.

Two distinct types of thickness dependence are observed in these selected polymers. PS and PM6 display significant thickness-dependent activation energies (E_a), while E_a values of the other two low-T_g CPs were nearly thickness-independent when approaching room temperature (**Figure 3b**). This observation is expected, as the heterogeneity of chain dynamics near the interface is larger for glassy films. The local relaxation time for polymer chains at the polymer/air interface can be several orders of magnitude lower than those chains far away from the interface. PS shows the highest E_a (140 kJ/mol) for films above 100 nm, which is lower than the previous bulk values from the literature (220 kJ/mol [61], 230 kJ/mol [62], and 350 kJ/mol [28]). Again, we attribute such depression to the influence of the soft polymer-water interface. Even if the ambient water does not fully penetrate the film, simulation results indicate that interfacial mobility dominates the overall thin film relaxation rate[20]. PFO-C10 has the lowest E_a of the other polymers, which is attributed to its near-amorphous morphology and a high fraction of low-T_g sidechains (**Table 1**). The E_a of PS and PM6 decreases linearly as film thickness reduces below approximately 100 nm. This result is in accordance with the well-documented confinement effect in polymer thin films.[63] A lack of physical barriers at the thin film interface can result in changes in dynamics due to the lower E_a

required for any polymer chain rearrangements. The E_a of PM6 is comparable to the range of E_a of other CPs measured by DMA[64].

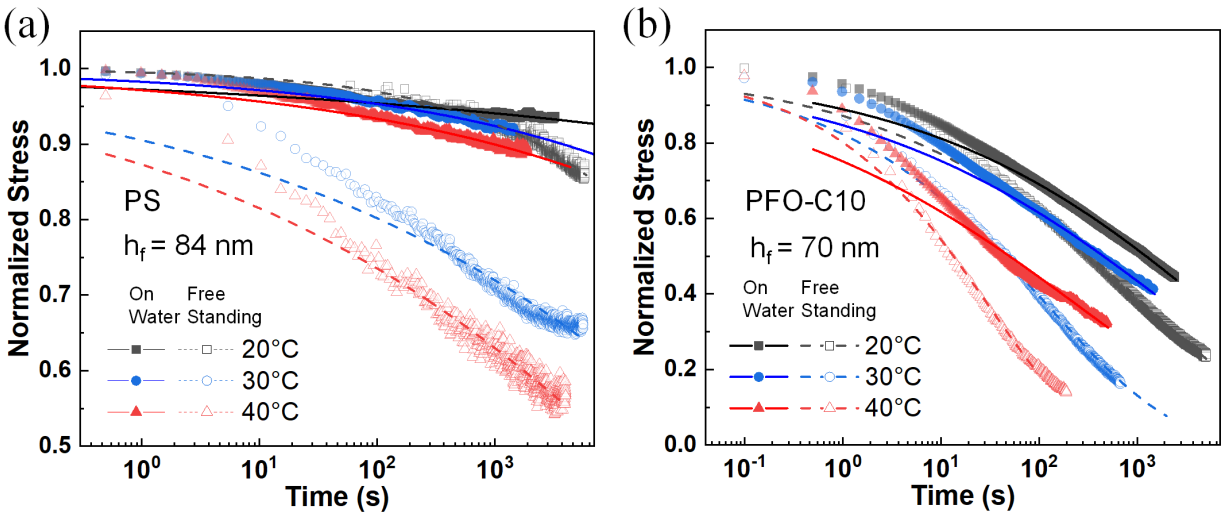

Figure 4 Stress relaxation of (a)PS and (b)PFO-C10 thin films measured by both film-on-water (filled symbols) and free-standing mode (open symbols), respectively. Continuous and dashed lines represent fitting curves for on-water and free-standing test results, respectively.

Stress relaxation tests were also performed on fully free-standing PS and PFO-C10 thin films to remove the possible effect of water (**Figure 4**). The free-standing polymer samples were transferred from the water surface to fully freely standing in the air by an established SMART transfer method.[39] A similar technique has been used to transfer PS thin film by Crosby group.[65-66] It was observed that for both polymers, free-standing films relaxed faster than films floated on the water at the same temperature. For example, for 84 nm PS films under 20 °C, the ⟨τ⟩ showed almost 9 orders of magnitude reduction in free-standing films when compared with film floating on water (**Figure 4a**). This acceleration phenomenon results from extra polymer-air interfaces for free-standing films. Those two highly mobile air polymer interfaces will greatly enhance the

overall relaxation rate in the thin film. Such enhancement effect decreases as temperature increases from 20 ℃ to 40 ℃, which is expected since the chain mobility heterogeneity decreases as temperature increases in glassy film. Thus, we do not expect similar relaxation enhancement will happen in low-T_g polymers like PFO-C10. As shown in **Figure 4b**, the free-standing film relaxes faster than films floated on the water at the same temperature, but the temperature dependence on relaxation kinetics is smaller (**Figure S10**). Overall, through the comparison of thin-film relaxation behaviors in the air and on the water surface, the effect of the polymer-air interface is verified, which will accelerate the relaxation rate in thin films. Meanwhile, such an enhancement in the thin film relaxation is more pronounced in the high-T_g system.

Conclusion

Here, we performed direct mechanical stress relaxation tests on both pseudo-free-standing and free-standing polymer thin films with PS, PM6, PFO-C10, and PDPP-TT. A stretched exponential equation was successfully applied to quantify the relaxation kinetics for tensile-drawn films. We observed an apparent thickness-dependent relaxation rate, i.e., the average relaxation time of PS film supported by water showed eight orders of magnitude reduction when thickness decreases from 84 nm to 58 nm at 20 ℃. It was also observed that the relaxation kinetics follows an Arrhenius-type temperature dependence. A converging trend was shown in the Arrhenius plot for thin films with different thicknesses, where the common temperature was lower than the bulk T_g. (40 ℃ lower for PS and 80 ℃ lower for PM6). Such relaxation enhancements were attributed to the increased dynamics of thin films at the polymer-water interface from the liquid water substrate. In other low-T_g conjugated polymers, the thickness-dependent relaxation rate was also observed, but they showed thickness-independent activation energy, indicating a less heterogenetic dynamics

nature in low T_g films. Furthermore, we compared the relaxation rate between these CPs, which all relax faster than PS at the same condition, and we found that PFO-C10 has the fastest relaxation rate due to its amorphous morphology compared with semicrystalline PDPP-TT despite PFO-C10 having a higher T_g. We also conducted the thin film relaxation on free-standing mode on PS and PFO-C10 as a comparison to films-on-water, and we found that the relaxation process is more sensitive to two polymer-air interfaces in high T_g PS film than low T_g PFO-C10.

It can be clearly seen from this work that the thin-film relaxation rate is influenced by thickness, temperature, and substrate. For CPs, the interplay of backbone T_g, volume fracture of low T_g sidechains, modulus, and morphology-related crystallization all contribute to the stress relaxation of thin films, and the deconvolution requires dedicated chemical structures and processing methods. Due to the significant stress relaxation behavior for CPs, future work should consider how to remediate such rapid stress change. For example, using crosslinked polymers, polymer blends, or bilayer systems to inhibit the relaxation of CPs active layer and improve long-term stability.

AUTHOR INFORMATION

Corresponding Author

*E-mail: Xiaodan.Gu@usm.edu

Author Contributions

X.G. conceived and directed the project. The mechanical relaxation test was done and analyzed by G.M, with assistance from S.Z. and L.G. The manuscript was drafted by G.M. with everyone's input. All authors have approved the final version of the manuscript.

Acknowledgment

This work was supported by Office of Naval Research under the award number N00014-23-1-2063. The setup of the thin film tensile testing tool was enabled by National Science Foundation under the award number DMR- 2047689. We thank Azoulay research group for providing PFO polymers.

Notes

The authors declare no competing financial interest.

References

(1) Bao, Z.; Chen, X. Flexible and Stretchable Devices. *Adv. Mater.* **2016,** *28* (22), 4177-4179, DOI: 10.1002/adma.201601422.

(2) Wang, M.; Baek, P.; Akbarinejad, A.; Barker, D.; Travas-Sejdic, J. Conjugated polymers and composites for stretchable organic electronics. *J. Mater. Chem. C* **2019,** *7* (19), 5534-5552, DOI: 10.1039/c9tc00709a.

(3) Gu, X.; Zhou, Y.; Gu, K.; Kurosawa, T.; Guo, Y.; Li, Y.; Lin, H.; Schroeder, B. C.; Yan, H.; Molina-Lopez, F.; Tassone, C. J.; Wang, C.; Mannsfeld, S. C. B.; Yan, H.; Zhao, D.; Toney, M. F.; Bao, Z. Roll-to-Roll Printed Large-Area All-Polymer Solar Cells with 5% Efficiency Based on a Low Crystallinity Conjugated Polymer Blend. *Adv. Energy Mater.* **2017,** *7* (14), 1602742, DOI: 10.1002/aenm.201602742.

(4) Bin, H.; Yang, Y.; Peng, Z.; Ye, L.; Yao, J.; Zhong, L.; Sun, C.; Gao, L.; Huang, H.; Li, X.; Qiu, B.; Xue, L.; Zhang, Z.-G.; Ade, H.; Li, Y. Effect of Alkylsilyl Side-Chain Structure on Photovoltaic Properties of Conjugated Polymer Donors. *Adv. Energy Mater.* **2018,** *8* (8), DOI: 10.1002/aenm.201702324.

(5) Melenbrink, E. L.; Hilby, K. M.; Choudhary, K.; Samal, S.; Kazerouni, N.; McConn, J. L.; Lipomi, D. J.; Thompson, B. C. Influence of Acceptor Side-Chain Length and Conjugation-Break Spacer Content on the Mechanical and Electronic Properties of Semi-Random Polymers. *ACS Appl. Polym. Mater.* **2019,** *1* (5), 1107-1117, DOI: 10.1021/acsapm.9b00115.

(6) Zhang, S.; Alesadi, A.; Selivanova, M.; Cao, Z.; Qian, Z.; Luo, S.; Galuska, L.; Teh, C.; Ocheje, M. U.; Mason, G. T.; St. Onge, P. B. J.; Zhou, D.; Rondeau-Gagné, S.; Xia, W.; Gu, X. Toward the Prediction and Control of Glass Transition Temperature for Donor–Acceptor Polymers. *Adv. Funct. Mater.* **2020,** *30* (27), DOI: 10.1002/adfm.202002221.

(7) Qian, Z.; Cao, Z.; Galuska, L.; Zhang, S.; Xu, J.; Gu, X. Glass Transition Phenomenon for Conjugated Polymers. *Macromol. Chem. Phys.* **2019,** *220* (11), DOI: 10.1002/macp.201900062.

(8) Li, Y.; Tatum, W. K.; Onorato, J. W.; Zhang, Y.; Luscombe, C. K. Low Elastic Modulus and High Charge Mobility of Low-Crystallinity Indacenodithiophene-Based Semiconducting Polymers for Potential Applications in Stretchable Electronics. *Macromolecules* **2018,** *51* (16), 6352-6358, DOI: 10.1021/acs.macromol.8b00898.

(9) Zhan, P. F.; Zhang, W. L.; Jacobs, I. E.; Nisson, D. M.; Xie, R. X.; Weissen, A. R.; Colby, R. H.; Moule, A. J.; Milner, S. T.; Maranas, J. K.; Gomez, E. D. Side Chain Length Affects Backbone Dynamics in Poly(3-Alkylthiophene)s. *J Polym Sci Pol Phys* **2018,** *56* (17), 1193-1202, DOI: 10.1002/polb.24637.

(10) Sugiyama, F.; Kleinschmidt, A. T.; Kayser, L. V.; Rodriquez, D.; Finn, M.; Alkhadra, M. A.; Wan, J. M. H.; Ramírez, J.; Chiang, A. S. C.; Root, S. E.; Savagatrup, S.; Lipomi, D. J. Effects of flexibility and branching of side chains on the mechanical properties of low-bandgap conjugated polymers. *Polym. Chem.* **2018,** *9* (33), 4354-4363, DOI: 10.1039/c8py00820e.

(11) Qian, Z.; Luo, S.; Qu, T.; Galuska, L. A.; Zhang, S.; Cao, Z.; Dhakal, S.; He, Y.; Hong, K.; Zhou, D.; Gu, X. Influence of side-chain isomerization on the isothermal crystallization kinetics of poly(3-alkylthiophenes). *J. Mater. Res.* **2020**, 1-12, DOI: 10.1557/jmr.2020.219.

(12) Kim, J. H.; Jang, J.; Zin, W. C. Estimation of the thickness dependence of the glass transition temperature in various thin polymer films. *Langmuir* **2000,** *16* (9), 4064-4067, DOI: DOI 10.1021/la991618t.

(13) Campoy-Quiles, M.; Sims, M.; Etchegoin, P. G.; Bradley, D. D. C. Thickness-dependent thermal transition temperatures in thin conjugated polymer films. *Macromolecules* **2006,** *39* (22), 7673-7680, DOI: 10.1021/ma0605752.

(14) Keddie, J. L.; Jones, R. A. L.; Cory, R. A. Size-Dependent Depression of the Glass-Transition Temperature in Polymer-Films. *Europhys. Lett.* **1994,** *27* (1), 59-64, DOI: Doi 10.1209/0295-5075/27/1/011.

(15) Mundra, M. K.; Ellison, C. J.; Behling, R. E.; Torkelson, J. M. Confinement, composition, and spin-coating effects on the glass transition and stress relaxation of thin films of polystyrene and styrene-containing random copolymers: Sensing by intrinsic fluorescence. *Polymer* **2006,** *47* (22), 7747-7759, DOI: 10.1016/j.polymer.2006.08.064.

(16) Chang, J.; Toga, K. B.; Paulsen, J. D.; Menon, N.; Russell, T. P. Thickness Dependence of the Young's Modulus of Polymer Thin Films. *Macromolecules* **2018,** *51* (17), 6764-6770, DOI: 10.1021/acs.macromol.8b00602.

(17) Paeng, K.; Swallen, S. F.; Ediger, M. D. Direct measurement of molecular motion in freestanding polystyrene thin films. *J Am Chem Soc* **2011,** *133* (22), 8444-7, DOI: 10.1021/ja2022834.

(18) Ediger, M. D. Spatially heterogeneous dynamics in supercooled liquids. *Annu Rev Phys Chem* **2000,** *51*, 99-128, DOI: 10.1146/annurev.physchem.51.1.99.

(19) Ediger, M. D.; Forrest, J. A. Dynamics near Free Surfaces and the Glass Transition in Thin Polymer Films: A View to the Future. *Macromolecules* **2013,** *47* (2), 471-478, DOI: 10.1021/ma4017696.

(20) Hanakata, P. Z.; Douglas, J. F.; Starr, F. W. Interfacial mobility scale determines the scale of collective motion and relaxation rate in polymer films. *Nat Commun* **2014,** *5*, 4163, DOI: 10.1038/ncomms5163.

(21) Yang, Z.; Fujii, Y.; Lee, F. K.; Lam, C. H.; Tsui, O. K. Glass transition dynamics and surface layer mobility in unentangled polystyrene films. *Science* **2010,** *328* (5986), 1676-9, DOI: 10.1126/science.1184394.

(22) Zhou, Y. X.; Milner, S. T. Short-Time Dynamics Reveals T-g Suppression in Simulated Polystyrene Thin Films. *Macromolecules* **2017,** *50* (14), 5599-5610, DOI: 10.1021/acs.macromol.7b00921.

(23) Jones, R. L.; Kumar, S. K.; Ho, D. L.; Briber, R. M.; Russell, T. P. Chain Conformation in Ultrathin Polymer Films Using Small-Angle Neutron Scattering. *Macromolecules* **2001,** *34* (3), 559-567, DOI: 10.1021/ma001141o.

(24) Akabori, K.-i.; Tanaka, K.; Nagamura, T.; Takahara, A.; Kajiyama, T. Molecular Motion in Ultrathin Polystyrene Films: Dynamic Mechanical Analysis of Surface and Interfacial Effects. *Macromolecules* **2005,** *38* (23), 9735-9741, DOI: 10.1021/ma051143e.

(25) Xu, J.; Ding, L.; Chen, J.; Gao, S.; Li, L.; Zhou, D.; Li, X.; Xue, G. Sensitive Characterization of the Influence of Substrate Interfaces on Supported Thin Films. *Macromolecules* **2014,** *47* (18), 6365-6372, DOI: 10.1021/ma500864k.

(26) Nguyen, H. K.; Kawaguchi, D.; Tanaka, K. Effect of Molecular Architecture on Conformational Relaxation of Polymer Chains at Interfaces. *Macromol Rapid Commun* **2020,** *41* (21), e2000096, DOI: 10.1002/marc.202000096.

(27) Tsuruta, H.; Fujii, Y.; Kai, N.; Kataoka, H.; Ishizone, T.; Doi, M.; Morita, H.; Tanaka, K. Local Conformation and Relaxation of Polystyrene at Substrate Interface. *Macromolecules* **2012,** *45* (11), 4643-4649, DOI: 10.1021/ma3007202.

(28) Chung, J. Y.; Douglas, J. F.; Stafford, C. M. A wrinkling-based method for investigating glassy polymer film relaxation as a function of film thickness and temperature. *J Chem Phys* **2017,** *147* (15), 154902, DOI: 10.1063/1.5006949.

(29) Petek, E. S.; Katsumata, R. Thickness Dependence of Contact Angles in Multilayered Ultrathin Polymer Films. *Macromolecules* **2022,** *55* (17), 7556-7563, DOI: 10.1021/acs.macromol.2c01123.

(30) Lu, H.; Chen, W.; Russell, T. P. Relaxation of Thin Films of Polystyrene Floating on Ionic Liquid Surface. *Macromolecules* **2009,** *42* (22), 9111-9117, DOI: 10.1021/ma901789k.

(31) Zhang, S.; Ocheje, M. U.; Luo, S.; Ehlenberg, D.; Appleby, B.; Weller, D.; Zhou, D.; Rondeau-Gagne, S.; Gu, X. Probing the Viscoelastic Property of Pseudo Free-Standing Conjugated Polymeric Thin Films. *Macromol Rapid Commun* **2018,** *39* (14), e1800092, DOI: 10.1002/marc.201800092.

(32) Yang, C.; Takahashi, I. Unusual thickness relaxation of spin-coated polystyrene ultrathin films in the glassy state. *Polymer* **2020,** *186*, DOI: 10.1016/j.polymer.2019.121972.

(33) Hanakata, P. Z.; Pazmino Betancourt, B. A.; Douglas, J. F.; Starr, F. W. A unifying framework to quantify the effects of substrate interactions, stiffness, and roughness on the

dynamics of thin supported polymer films. *J Chem Phys* **2015,** *142* (23), 234907, DOI: 10.1063/1.4922481.

(34) Evans, C. M.; Deng, H.; Jager, W. F.; Torkelson, J. M. Fragility is a Key Parameter in Determining the Magnitude of Tg-Confinement Effects in Polymer Films. *Macromolecules* **2013,** *46* (15), 6091-6103, DOI: 10.1021/ma401017n.

(35) Wang, T.; Hu, S.; Zhang, S.; Peera, A.; Reffner, J.; Torkelson, J. M. Eliminating the Tg-Confinement Effect in Polystyrene Films: Extraordinary Impact of a 2 mol % 2-Ethylhexyl Acrylate Comonomer. *Macromolecules* **2022,** *55* (21), 9601-9611, DOI: 10.1021/acs.macromol.2c01917.

(36) Kerle, T.; Lin, Z.; Kim, H.-C.; Russell, T. P. J. M. Mobility of polymers at the air/polymer interface. **2001,** *34* (10), 3484-3492.

(37) Chan, E. P.; Kundu, S.; Lin, Q.; Stafford, C. M. Quantifying the stress relaxation modulus of polymer thin films via thermal wrinkling. *ACS Appl Mater Interfaces* **2011,** *3* (2), 331-8, DOI: 10.1021/am100956q.

(38) Kim, T.; Kim, J.-H.; Kang, T. E.; Lee, C.; Kang, H.; Shin, M.; Wang, C.; Ma, B.; Jeong, U.; Kim, T.-S. Flexible, highly efficient all-polymer solar cells. *Nat Commun* **2015,** *6* (1), 1-7, DOI: 10.1038/ncomms9547.

(39) Galuska, L. A.; Muckley, E. S.; Cao, Z.; Ehlenberg, D. F.; Qian, Z.; Zhang, S.; Rondeau-Gagne, S.; Phan, M. D.; Ankner, J. F.; Ivanov, I. N.; Gu, X. SMART transfer method to directly compare the mechanical response of water-supported and free-standing ultrathin polymeric films. *Nat Commun* **2021,** *12* (1), 2347, DOI: 10.1038/s41467-021-22473-w.

(40) Donnelly, V. M.; Kornblit, A. Plasma etching: Yesterday, today, and tomorrow. *Journal of Vacuum Science & Technology A: Vacuum, Surfaces, and Films* **2013,** *31* (5), DOI: 10.1116/1.4819316.

(41) Ma, B. S.; Lee, J.-W.; Park, H.; Kim, B. J.; Kim, T.-S. Thermomechanical Behavior of Poly(3-hexylthiophene) Thin Films on the Water Surface. *ACS Omega* **2022,** *7* (23), 19706-19713, DOI: 10.1021/acsomega.2c01451.

(42) Johnston, I. D.; McCluskey, D. K.; Tan, C. K. L.; Tracey, M. C. Mechanical characterization of bulk Sylgard 184 for microfluidics and microengineering. *J. Micromech. Microeng.* **2014,** *24* (3), 035017, DOI: 10.1088/0960-1317/24/3/035017.

(43) Zhang, S.; Ocheje, M. U.; Huang, L.; Galuska, L.; Cao, Z.; Luo, S.; Cheng, Y. H.; Ehlenberg, D.; Goodman, R. B.; Zhou, D.; Liu, Y.; Chiu, Y. C.; Azoulay, J. D.; Rondeau-Gagné, S.; Gu, X. The Critical Role of Electron-Donating Thiophene Groups on the Mechanical and Thermal Properties of Donor–Acceptor Semiconducting Polymers. *Adv. Electron. Mater.* **2019,** *5* (5), DOI: 10.1002/aelm.201800899.

(44) Angell, C. A.; Ngai, K. L.; McKenna, G. B.; McMillan, P. F.; Martin, S. W. Relaxation in glassforming liquids and amorphous solids. *J. Appl. Phys.* **2000,** *88* (6), 3113-3157, DOI: 10.1063/1.1286035.

(45) Ghasemi, M.; Balar, N.; Peng, Z.; Hu, H.; Qin, Y.; Kim, T.; Rech, J. J.; Bidwell, M.; Mask, W.; McCulloch, I.; You, W.; Amassian, A.; Risko, C.; O'Connor, B. T.; Ade, H. A molecular interaction-diffusion framework for predicting organic solar cell stability. *Nat. Mater.* **2021,** *20* (4), 525-532, DOI: 10.1038/s41563-020-00872-6.

(46) Mauro, J. C.; Mauro, Y. Z. On the Prony series representation of stretched exponential relaxation. *Physica A* **2018,** *506*, 75-87, DOI: 10.1016/j.physa.2018.04.047.

(47) Kim, S.; Hewlett, S. A.; Roth, C. B.; Torkelson, J. M. Confinement effects on glass transition temperature, transition breadth, and expansivity: comparison of ellipsometry and fluorescence measurements on polystyrene films. *Eur Phys J E Soft Matter* **2009,** *30* (1), 83-92, DOI: 10.1140/epje/i2009-10510-y.

(48) Lee, H. N.; Paeng, K.; Swallen, S. F.; Ediger, M. D.; Stamm, R. A.; Medvedev, G. A.; Caruthers, J. M. Molecular Mobility of Poly(methyl methacrylate) Glass During Uniaxial Tensile Creep Deformation. *J Polym Sci Pol Phys* **2009,** *47* (17), 1713-1727, DOI: 10.1002/polb.21774.

(49) Johnston, D. C. Stretched exponential relaxation arising from a continuous sum of exponential decays. *Physical Review B* **2006,** *74* (18), DOI: 10.1103/PhysRevB.74.184430.

(50) Qi, D.; Ilton, M.; Forrest, J. A. Measuring surface and bulk relaxation in glassy polymers. *Eur Phys J E Soft Matter* **2011,** *34* (6), 56, DOI: 10.1140/epje/i2011-11056-1.

(51) O'Connell, P. A.; McKenna, G. B. Arrhenius-type temperature dependence of the segmental relaxation below T-g. *J. Chem. Phys.* **1999,** *110* (22), 11054-11060, DOI: Doi 10.1063/1.479046.

(52) Fakhraai, Z.; Forrest, J. A. Probing slow dynamics in supported thin polymer films. *Phys Rev Lett* **2005,** *95* (2), 025701, DOI: 10.1103/PhysRevLett.95.025701.

(53) Dhinojwala, A.; Wong, G. K.; Torkelson, J. M. Rotational reorientation dynamics of disperse red 1 in polystyrene: α -relaxation dynamics probed by second harmonic generation and dielectric relaxation. *The Journal of Chemical Physics* **1994,** *100* (8), 6046-6054, DOI: 10.1063/1.467115.

(54) Dyre, J. C. A Phenomenological Model for the Meyer-Neldel Rule. *Journal of Physics C-Solid State Physics* **1986,** *19* (28), 5655-5664, DOI: Doi 10.1088/0022-3719/19/28/016.

(55) DeMaggio, G. B.; Frieze, W. E.; Gidley, D. W.; Zhu, M.; Hristov, H. A.; Yee, A. F. Interface and Surface Effects on the Glass Transition in Thin Polystyrene Films. *Phys. Rev. Lett.* **1997,** *78* (8), 1524-1527, DOI: 10.1103/PhysRevLett.78.1524.

(56) Smith, E. G.; Robb, I. D. N.m.r. studies on the effect of water on the glass transition of polystyrene. *Polymer* **1974,** *15* (11), 713-716, DOI: 10.1016/0032-3861(74)90022-6.

(57) Zhang, W.; Douglas, J. F.; Starr, F. W. Why we need to look beyond the glass transition temperature to characterize the dynamics of thin supported polymer films. *PNAS* **2018,** *115* (22), 5641-5646, DOI: 10.1073/pnas.1722024115.

(58) Schroeder, B. C.; Kurosawa, T.; Fu, T.; Chiu, Y.-C.; Mun, J.; Wang, G.-J. N.; Gu, X.; Shaw, L.; Kneller, J. W. E.; Kreouzis, T.; Toney, M. F.; Bao, Z. Taming Charge Transport in Semiconducting Polymers with Branched Alkyl Side Chains. *Adv. Funct. Mater.* **2017,** *27* (34), DOI: 10.1002/adfm.201701973.

(59) Xu, X.; Douglas, J. F.; Xu, W.-S. Influence of Side-Chain Length and Relative Rigidities of Backbone and Side Chains on Glass Formation of Branched Polymers. *Macromolecules* **2021,** *54* (13), 6327-6341, DOI: 10.1021/acs.macromol.1c00834.

(60) Savagatrup, S.; Makaram, A. S.; Burke, D. J.; Lipomi, D. J. Mechanical Properties of Conjugated Polymers and Polymer-Fullerene Composites as a Function of Molecular Structure. *Adv. Funct. Mater.* **2014,** *24* (8), 1169-1181, DOI: 10.1002/adfm.201302646.

(61) Plazek, D. J.; Ngai, K. L. Correlation of Polymer Segmental Chain Dynamics with Temperature-Dependent Time-Scale Shifts. *Macromolecules* **1991,** *24* (5), 1222-1224, DOI: DOI 10.1021/ma00005a044.

(62) Tanaka, K.; Takahara, A.; Kajiyama, T. Rheological Analysis of Surface Relaxation Process of Monodisperse Polystyrene Films. *Macromolecules* **2000,** *33* (20), 7588-7593, DOI: 10.1021/ma000406w.

(63) Lee, J.-H.; Chung, J. Y.; Stafford, C. M. Effect of Confinement on Stiffness and Fracture of Thin Amorphous Polymer Films. *ACS Macro Lett.* **2011,** *1* (1), 122-126, DOI: 10.1021/mz200090a.

(64) Balar, N.; Siddika, S.; Kashani, S.; Peng, Z.; Rech, J. J.; Ye, L.; You, W.; Ade, H.; O'Connor, B. T. Role of Secondary Thermal Relaxations in Conjugated Polymer Film Toughness. *Chem. Mater.* **2020,** *32* (15), 6540-6549, DOI: 10.1021/acs.chemmater.0c01910.

(65) Bay, R. K.; Zarybnicka, K.; Jančář, J.; Crosby, A. J. Mechanical Properties of Ultrathin Polymer Nanocomposites. *ACS Appl. Polym. Mater.* **2020,** *2* (6), 2220-2227, DOI: 10.1021/acsapm.0c00201.

(66) Bay, R. K.; Crosby, A. J. Uniaxial Extension of Ultrathin Freestanding Polymer Films. *ACS Macro Lett* **2019,** *8* (9), 1080-1085, DOI: 10.1021/acsmacrolett.9b00408.

TOC Figure

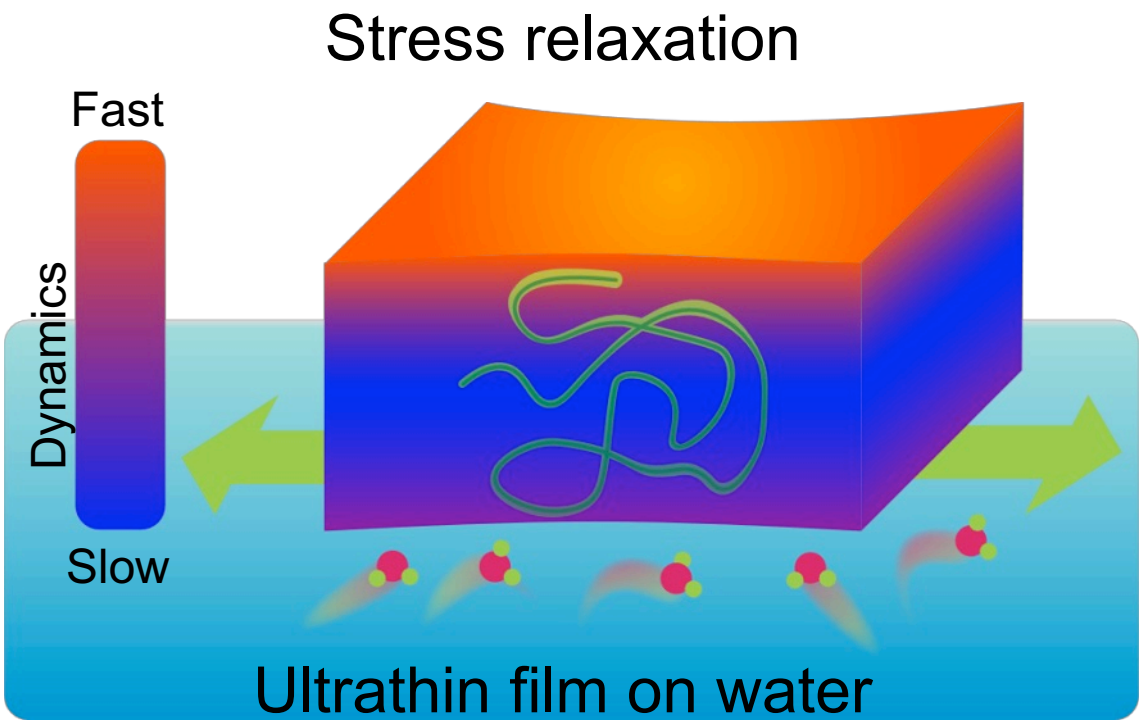
Stress relaxation
Fast
Dynamics
Slow
Ultrathin film on water